Journal of Inorganic Biochemistry 193 (2019) 84–93

Contents lists available at ScienceDirect

Journal of Inorganic Biochemistry

journal homepage: www.elsevier.com/locate/jinorgbio

An in vitro study on dentin demineralization and remineralization: Collagen rearrangements and influence on the enucleated phase

Michele Di Foggia[a], Carlo Prati[b], Maria Giovanna Gandolfi[c], Paola Taddei[a,*]

[a] Biochemistry Unit, Department of Biomedical and Neuromotor Sciences, University of Bologna, Via Belmeloro 8/2, 40126 Bologna, Italy
[b] Endodontic Clinical Section, Unit of Odontostomatological Sciences, Department of Biomedical and Neuromotor Sciences, University of Bologna, Via San Vitale 59, 40136 Bologna, Italy
[c] Laboratory of Biomaterials and Oral Pathology, Unit of Odontostomatological Sciences, Department of Biomedical and Neuromotor Sciences, University of Bologna, Via San Vitale 59, 40136 Bologna, Italy

ARTICLE INFO

Keywords:
Dentin
Collagen
Secondary structure
Calcium-releasing cements
Remineralization
Vibrational spectroscopy

ABSTRACT

Dentin remineralization is of clinical relevance in the therapy of caries and dentin hypersensitivity. This study is aimed at gaining more insights on a molecular scale, through IR spectroscopy, into dentin demineralization and remineralization. The dentin demineralization by ethylenediaminetetraacetic acid, EDTA (17%, 2 h) significantly altered the secondary structure distribution of collagen, upon loss of interaction with calcium ions. To investigate dentin remineralization, previously demineralized human dentin slices were soaked in Dulbecco's Phosphate Buffered Saline (DPBS) or Hank's Balanced Salt Solution HBSS, in close contact with three commercial cements used as sustained releasing sources of Ca^{2+} and OH^{-} ions (i.e. calcium hydroxide- and calcium silicate-based cements). IR spectroscopy showed the occurrence of remineralization under these conditions. Collagen did not lose its ability to chelate Ca^{2+}, and these interactions allowed collagen to rearrange into a conformation similar to that of sound dentin. This process appeared slower in HBSS than DPBS, as also shown by the lower degree of maturation of the inorganic phase enucleated in the former medium (amorphous calcium phosphate versus B-type carbonated apatite). Collagen appeared to act as a spatial constraint to crystal deposition, affecting crystallinity and carbonate content of the enucleated phase. Remineralization was found to strongly depend on the calcium releasing ability of the cements. The fast formation of a rough apatite biocoating may represent a favorable clinical condition in the context of mineralized tissue regeneration.

1. Introduction

Biomineralization is an organic matrix-mediated process in which organic macromolecules act as templates for the nucleation and growth of mineral crystals to form hierarchically ordered hybrid materials such as bone or teeth. Molecular interactions play a key-role in the crystallographic control over the oriented nucleation at the matrix-mineral interface. Mineral ions interact with the organic matrix to produce crystallographically oriented hybrid nanostructures [1].

In dentin mineralization, type I collagen, the main matrix protein (accounting for about 90% of the organic phase), acts as a template for mineral deposition in the presence of non-collagenous proteins, NCP (such as dentin matrix protein, DMP1, and dentin phosphoprotein DPP). NCP are thought to provide the driving force required to reduce the activation energy of nucleation and formation of apatite [2,3]. Some of these macromolecules often contain aspartic acid, glutamic acid, phosphorylated serine and threonine, so that they are believed to be involved in mineral deposition thanks to their high affinity for Ca^{2+} and collagen. Also the phosphorylation degree of these proteins has proved to play a significant role in mineralization inhibition and induction [4].

Dentin remineralization is of clinical relevance in the therapy of dental caries and dentin hypersensitivity. In dental caries, the initial carious lesion reduces the crystallinity, carbonate and magnesium contents and crystal orientation of the inorganic phase of dentin [5] and exposes collagen fibres, leading to the rapid destruction of the dentin network, with consequent risk for pulp exposure and bacterial contamination. Treatment typically involves remineralization of caries-affected dentin. Several biomimetic strategies have been developed to achieve remineralization of collagen, inspired by the behavior of the protein matrix in biomineralization processes [6–11]. They included treatment with phosphorylated chitosan [6], polyanionic agarose [7], polyvinylphosphonic acid/polyacrylic acid biomimetic analogues [8,10], peptides containing phosphoserine and carboxylate groups [9],

* Corresponding author.
E-mail address: paola.taddei@unibo.it (P. Taddei).

https://doi.org/10.1016/j.jinorgbio.2019.01.004
Received 12 July 2018; Received in revised form 24 December 2018; Accepted 10 January 2019
Available online 18 January 2019
0162-0134/

poly(allylamine)- and poly(aspartic acid)-stabilized amorphous calcium phosphate (ACP) [11].

Calcium hydroxide-, calcium oxide- and calcium silicate-based materials (mineral trioxide aggregate, MTA, and other Portland cements) may be used as sustained releasing sources of Ca^{2+} and OH^- ions. Calcium silicate cements proved the ability to create a suitable bioactive surface with an appropriate architecture thanks to the nucleation of calcium phosphate deposits and the formation of an apatite layer [12–14], whose kinetics has been extensively investigated in vitro [15,16] and in vivo [17]. The apatite forming ability offers many advantages such as the exposure of a suitable surface for cells [18]. Calcium release enhances the activity of pulpal cells and osteoblasts [19,20], and plays a positive role in promoting differentiation and in stimulating dentinogenesis, osteogenesis and cementogenesis [17,21,22]. Moreover, it favors the formation of a dentin bridge [23,24]; hence, the adjacent dentin may be remineralized through the deposition of apatite crystals [10].

This study is aimed at gaining more insights on a molecular scale into demineralization and remineralization of dentin. Demineralization was achieved through ethylenediaminetetraacetic acid (EDTA) treatment, with the aim of reproducing the typical conditions created by the endodontic therapy, rather than to mimic a caries lesion. Actually, this procedure is usually used in endodontics to demineralize dentin, remove the smear layer coating and open dentinal tubules [25,26]. Dentin collagen rearrangements upon demineralization have been investigated through IR spectroscopy in the Attenuated Total Reflectance (ATR) mode, commonly used for the non-destructive characterization of mineralized tissues [27]. The same technique was used to ascertain if the conformational changes induced in collagen by the adopted demineralizing conditions prevented calcium chelation and thus remineralization. To this aim, demineralized dentin slices were aged in Dulbecco's Phosphate Buffered Saline (DPBS) or Hank's Balanced Salt Solution (HBSS), used as simulated body fluids (SBFs), in presence of three commercial materials (i.e. TheraCal, ProRoot MTA and Dycal), chosen for their ability to release Ca^{2+} and OH^- ions [28]. The influence of the SBF medium as well as of collagen on the enucleated phase was investigated. Infrared spectroscopy is a well-established technique for the analysis of the secondary structure of proteins and polypeptides [29,30]. It has been chosen and preferred to other techniques [31] because of its non-invasive character. Actually, it allows the analysis of solid samples, such as the dentin slices under study, without any significant manipulation, i.e. with the certainty that the detected changes were effectively due to the investigated treatments rather than to sample preparation.

2. Materials and methods

2.1. Calcium-releasing cements

Dycal (i.e. a conventional calcium hydroxide-based cement), TheraCal (i.e. a light-curable resin-based Portland cement-containing material) and White ProRoot MTA (i.e. a self-setting calcium silicate MTA cement) were used as sustained releasing sources of Ca^{2+} and OH^- ions, [28]. Dycal (lot. 081007, Dentsply, USA) is a two-paste self-setting system formed by a base paste (1,3-butylene glycol disalicylate, zinc oxide, calcium phosphate, calcium tungstate, iron oxide pigments) and a catalyst paste (calcium hydroxide, *N*-ethyl-o/p-toluene sulphonamide, zinc oxide, titanium oxide, zinc stearate, iron oxide pigments). TheraCal (lot. 603-189-A, Bisco Inc., USA) is a single paste ready for use; it is a light-cured resin-modified calcium silicate-filled base/liner material containing approximately 45% wt mineral material (type III Portland cement), 10% wt radiopaque component, 5% wt hydrophilic thickening agent (fumed silica) and approximately 45% resin. The resin consists of a hydrophobic component (comprising hydrophobic monomers) such as urethane dimethacrylate (UDMA), bisphenol A-glycidyl methacrylate (BisGMA), triethylene glycol dimethacrylate (TEGDMA) and a hydrophilic component (containing hydrophilic monomers) such as hydroxyethyl methacrylate (HEMA) and polyethylene glycol dimethacrylate (PEGDMA). White ProRoot MTA (lot. 09001920, Dentsply, USA) is a self-setting hydrophilic hydroxide-releasing cement, mainly composed of Portland cement and bismuth oxide.

All materials were prepared according to the manufacturers' directions. They were compacted to excess into polyvinyl chloride (PVC) cylindrical molds (8 mm diameter, 1.6 mm thick). Dycal and ProRoot MTA were cured (37 °C, 98% relative humidity) for a period corresponding to 70% of the final setting time, i.e. 2 and 117 min, respectively, and then demolded. The final setting time has been evaluated using a Gilmore-type metric indenter, having a mass of 100.0 ± 0.5 g and a flat end of diameter 2.0 ± 0.1 mm. The needle tip shall be cylindrical over a distance of at least 5 mm, following ISO 6876 Dental root canal sealing materials. The end of the needle shall be plane and at right angles to the longitudinal axis. When the setting time stated by the manufacturer approached, the Gilmore-type indenter was carefully lowed vertically on the horizontal surface of the material. If an indentation was visible, the needle was raised and the needle tip cleaned, and the needle was lowered to a new position on the surface of the material. This operation was repeated until no indentation mark was visible. The final setting time was the period elapsed between the end of mixing and the absence of indentation mark. Immediately after insertion in the mould, TheraCal samples were light-cured with a halogen lamp (T-LED elca, Anthos Cefla, Imola, Italy) for 20 s on both surfaces through a transparent polyester strip and then demolded.

2.2. Dentin demineralization and remineralization tests

Human dentin slices (5 ± 2 mm side and 0.8 ± 0.1 mm thick) from molar teeth extracted for orthodontic/surgical reasons, were prepared and demineralized in 15 mL of EDTA 17% for 2 h at room temperature, as previously reported [32]. This treatment is known to remove the main part of NCP as well as the inorganic phase of dentin [33]. The dentin slices were analyzed by ATR-IR and Raman spectroscopy before and after EDTA treatment.

Disks of the three cements were prepared as previously described, and were used immediately after preparation for the dentin remineralization tests. Each material disk was maintained in close contact with a demineralized dentin slice using a tailored PVC support. In the first experiment, the cements were soaked in 15 mL of DPBS at 37 °C for 7 days in a polystyrene sealed container. The second experiment was carried out in HBSS for 14 days, i.e. for a longer time due to slower calcium phosphate deposition in HBSS [16]. In control group, demineralized dentin slices were soaked without any cement for 14 days in HBSS or in a metastable calcifying medium containing Ca^{2+} and PO_4^{3-} ions (Ca/P ratio = 1.67, pH 7.3), according to Chirila et al. [34]. After the experiments, each dentin slice was rinsed with deionized water and then analyzed by ATR-IR spectroscopy. The aged cement disks were analyzed as well.

2.3. Vibrational ATR-IR and Raman and spectroscopic analyses

IR spectra were recorded on a Nicolet 5700 Fourier Transform FT-IR (Thermo Electron Scientific Instruments Corp., Madison, WI, USA), equipped with a smart orbit diamond ATR accessory and a deuterated triglycine sulphate (DTGS) detector; the spectral resolution was 4 cm^{-1}. FT-Raman spectra were recorded on a Bruker MultiRam FT-Raman spectrometer equipped with a cooled Ge-diode detector. The excitation source was a neodymium-doped yttrium aluminum garnet (Nd^{3+}-YAG) laser (1064 nm) in the backscattering configuration. The focused laser beam diameter was about 100 µm, with a power at the sample of about 200 mW. Spectral resolution was 4 cm^{-1}. To minimize the variability deriving from possible sample inhomogeneity, three spectra at least were recorded on three different points of each sample. The IR-ATR technique has been chosen to gain insights into the surface composition

of the dentin slices at each step of the study (under the used experimental conditions, the investigated sample thickness was about 2 μm). FT-Raman spectroscopy was used to ascertain the only partial demineralization of dentin slices, being this technique sensitive to the sample bulk.

According to Du et al. [35], the collagen $I_{Amide\ II}/I_{Amide\ I}$ IR ratio (where $I_{Amide\ II}$ and $I_{Amide\ I}$ were the maximum peak heigths of the Amide II and Amide I bands, respectively) was calculated to investigate the possible changes in hydrogen bonding interactions and crosslinking. The ratio was calculated as peak height rather than as peak area due to the superposition of the carbonate stretching band of B-type carbonated apatite to the Amide II band profile. The collagen $I_{Amide\ III}/I_{1450}$ IR ratio (where $I_{Amide\ III}$ and I_{1450} were the peak heights of the Amide III and 1450 cm^{-1} bands, respectively) was calculated according to other studies [36,37], to investigate the integrity of the collagen triple-helix upon demineralization. A value of 1 is generally obtained when the integrity of the triple-helix is not affected [35]. Unfortunately, this ratio was not reliable in mineralized collagen samples due to the contribution of the carbonate stretching band of B-type carbonated apatite to the 1450 cm^{-1} band.

As previously reported [32], the calcium phosphate (Ca/P)/collagen ratio was evaluated through the $I_{CaP}/I_{collagen}$ IR intensity ratio, where I_{CaP} and $I_{collagen}$ were the intensities as peak heights of the ν_3 PO_4^{3-} band and Amide I of collagen, respectively. The evaluation through peak height has been preferred over that using peak area [38], due to the unreliability of the area of the Amide I band for the dentin samples that stayed in contact with Dycal (see the Results section) because of the contribution of the salicylate bands. The $I_{CaP}/I_{collagen}$ IR intensity ratio may be used to assess the relative thickness of the apatite phase enucleated in the different remineralization tests. Although this ratio does not represent a measurement of the absolute thickness of the apatite phase, it allows a comparative evaluation between samples under the different used conditions. In fact, at increasing apatite thickness, the contribution of the collagen bands to the IR spectrum of the remineralized dentin sample progressively decreases, determining a progressive increase in the $I_{CaP}/I_{collagen}$ IR intensity ratio. The carbonate content of the B-type carbonated apatite phase was evaluated through the $I_{carbonate}/I_{phosphate}$ ratio, where $I_{carbonate}$ and $I_{phosphate}$ were the intensities as peak heights of the carbonate band at about 870 cm^{-1} and the ν_3 PO_4^{3-} band, respectively.

2.4. Statistical analysis

Data were analyzed applying the one-way ANOVA followed by Student-Newman-Keuls test using the Sisvar statistical software (Daniel Furtado Ferreira, Universidade Federal de Lavras/UFLA – Brazil). Statistical significance was set at $p < 0.05$.

3. Results

3.1. Dentin demineralization

Figs. 1 and 2 show the average IR and Raman spectra, respectively, recorded on the dentin slices before and after demineralization with EDTA 17% for 2 h. The bands assignable to collagen as well as to B-type carbonated apatite have been indicated according to the literature [36,39].

Upon the EDTA treatment, the IR bands assigned to the mineral phase disappeared while those of collagen underwent significant changes in intensity and wavenumber position with respect to sound dentin (Fig. 1). In particular, by normalizing the spectra to the intensity of the Amide A band at about 3280 cm^{-1}, the Amide I, II and III bands significantly increased in intensity upon demineralization. At the same time, the Amide I band noticeably changed its profile, with a wavenumber shift of its maximum from 1641 to 1628 cm^{-1}. To gain more insights into collagen secondary structure rearrangements induced by demineralization, the Amide I spectral range was analyzed by band fitting. Fig. S1, Supplementary Information shows the spectral components obtained by this procedure. The obtained percentages of secondary structure conformations are reported in Fig. 3. As can be easily seen, upon demineralization, the contents of β-sheet and unordered conformations increased while those of triple-helix, α-helix and β-turns decreased. Collagen conformational rearrangements were confirmed by the $I_{Amide\ II}/I_{Amide\ I}$ and $I_{Amide\ III}/I_{1450}$ ratios: upon EDTA treatment, the former increased from 0.79 ± 0.02 to 0.90 ± 0.02, the latter assumed a value of 0.81 ± 0.04 (i.e. lower than 1).

With regards to the Raman spectra (Fig. 2), upon demineralization under the utilized conditions, the bands assignable to B-type carbonated apatite weakened but did not disappear, differently from the IR spectra.

3.2. Dentin remineralization tests

3.2.1. Experiments in DPBS

Figs. 4, 5 and 6 show the average IR spectra recorded on the demineralized dentin slices that stayed in contact with TheraCal, ProRoot MTA and Dycal for 7 days in DPBS, respectively. The spectra of the aged material disks are reported for comparison.

All the demineralized dentin samples remineralized, as indicated by the appearance of the bands at about 1415 cm^{-1} (ν_3 CO_3^{2-} antisymmetric stretching in B-type carbonated apatites), 1012–1025 cm^{-1} (ν_3 PO_4^{3-} antisymmetric stretching), 960 cm^{-1} (ν_1 PO_4^{3-} symmetric stretching), 870 cm^{-1} (ν_2 CO_3^{2-} out-of-plane bending in B-type carbonated apatites), 600 and 560 cm^{-1} (ν_4 PO_4^{3-} out-of-plane bending) [39], assignable to a B-type carbonated apatite. These bands were superimposed to those of collagen in all the spectra.

In the case of the dentin slices that stayed in contact with Dycal, several bands (indicated with an asterisk) ascribable to the salicylate component were detected (Fig. 6). On the contrary, no bands due to the silicate component were detected on the dentin slices that stayed in contact either with TheraCal or ProRoot (Figs. 4(a) and 5(a)), suggesting that no deposition of a Si-containing matrix occurred. For these latter two samples, the bands of collagen underwent significant changes in wavenumber positions and intensity upon remineralization, with a trend opposite to that observed upon demineralization. In fact, upon remineralization, the Amide I, II and III bands weakened and the $I_{Amide\ II}/I_{Amide\ I}$ ratio decreased attaining values similar to those observed for sound dentin (Fig. 7(a)). Moreover, Amide I shifted to higher wavenumber and noticeably changed its spectral profile more resembling that observed for sound dentin (Figs. 4(b) and 5(b)). Unfortunately, no analogous considerations can be made for the dentin sample that stayed in contact with Dycal, due to the superposition of the salicylate bands on the Amide ones (Fig. 6). The qualitative considerations above reported for the dentin slices that were aged in contact with TheraCal and ProRoot MTA were confirmed by the Amide I band fitting data reported in Fig. 3(a) (see Fig. S2, Supplementary Information, for the fitted spectra). The obtained percentages of secondary structure conformations showed that upon remineralization the contents of triple-helix and β-sheet changed attaining values similar to those of sound dentin, while the amounts of the other conformations (in particular α-helix) were different.

To evaluate the relative thickness of the apatite deposit, the $I_{CaP}/I_{collagen}$ intensity ratio between the main apatite and collagen bands (i.e. the ν_3 PO_4^{3-} and Amide I, respectively) was calculated and the obtained data are reported in Fig. 7(b). Upon treatment with all the cements, the $I_{CaP}/I_{collagen}$ ratio increased with respect to demineralized dentin, to the highest extent with TheraCal (Fig. 7(b)). However, the B-type carbonated apatite phase formed upon contact with all the cements appeared different from that typical of sound dentin, as well as from that formed on the disks that stayed in contact with dentin in the ageing medium (Figs. 4(a), 5(a) and 6). As can be easily seen, both in remineralized dentin slices and cement disks, the ν_3 PO_4^{3-} mode fell at higher wavenumbers with respect to sound dentin. It may be observed

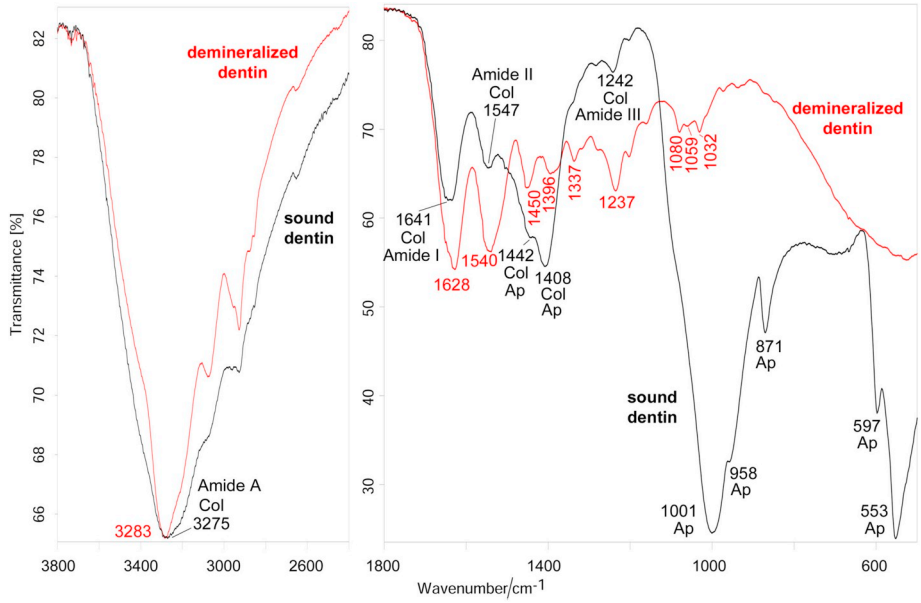

Fig. 1. Average IR spectra recorded on the dentin slices before and after demineralization with EDTA 17% for 2 h. The spectra were normalized to the intensity of the Amide A band at about 3280 cm^{-1}. The bands prevalently due to collagen (Col) and B-type carbonated apatite (Ap) are indicated.

that the B-type carbonated apatite formed on the remineralized dentin slices had a crystallinity similar to the inorganic phase of sound dentin (i.e. had a similar full-width at half maximum of the ν_3 PO_4^{3-} band, $FWHM_{phosphate}$, Fig. 7(c)), but was always less crystalline (i.e. had a higher $FWHM_{phosphate}$, Fig. 7(c)) than that deposited on the corresponding cement disk. Differences in carbonate contents were found as well (Fig. 7(d)): the amount of carbonate in the B-type carbonated apatite formed on remineralized dentin was always lower than that of sound dentin and, for the TheraCal treatment, also than that of the phase formed on the corresponding cement disk.

3.2.2. Experiments in HBSS

Figs. 8, 9 and 10 show the average IR spectra recorded on the demineralized dentin slices that stayed in contact with TheraCal, ProRoot MTA and Dycal for 14 days in HBSS, respectively. The spectra of the aged material disks are reported for comparison.

As can be easily seen from the spectra and from the $I_{CaP}/I_{collagen}$ data reported in Fig. 7(b), Dycal induced a negligible dentin remineralization, while TheraCal and ProRoot MTA displayed a significantly higher remineralizing ability (and comparable to each other). TheraCal induced the deposition of a B-type carbonated apatite deposit (Fig. 8), although it had lower thickness (i.e. lower $I_{CaP}/I_{collagen}$ Fig. 7(b)) and lower crystallinity (i.e. higher $FWHM_{phosphate}$, Fig. 7(c)) than in DPBS. It is interesting to note that the spectra of the dentin slices that stayed in contact with TheraCal showed a broad band at about 1720 cm^{-1}, ascribable to the C=O stretching mode of the resin (Fig. 8). ProRoot MTA induced the formation of a deposit containing calcite, aragonite and ACP (Fig. 9), with a $I_{CaP}/I_{collagen}$ ratio similar to that obtained in DPBS (Fig. 7(b)). The crystallinity of the phase formed on dentin upon the treatment with both TheraCal and ProRoot MTA was lower than that of

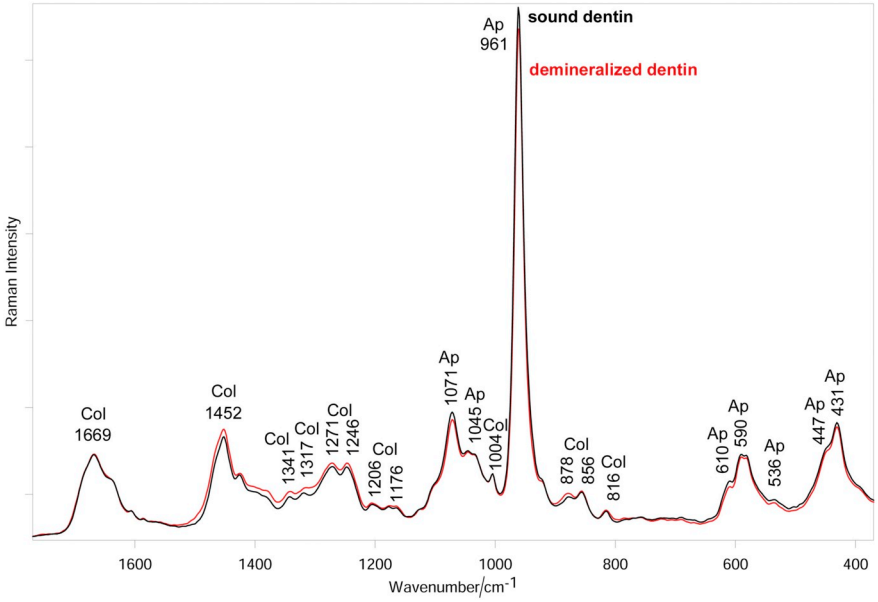

Fig. 2. Average Raman spectra recorded on the dentin slices before and after demineralization with EDTA 17% for 2 h. The spectra were normalized to the intensity of the Amide I band at 1669 cm^{-1}. The bands prevalently due to collagen (Col) and B-type carbonated apatite (Ap) are indicated.

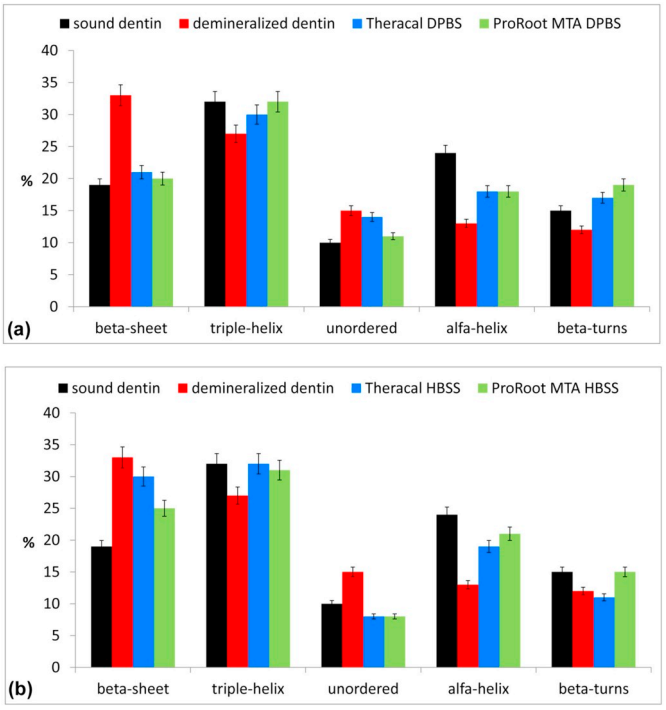

Fig. 3. (a) Percentages of secondary structure conformations as obtained by the curve fitting of the IR Amide I range of sound dentin, demineralized dentin slices before and after ageing in contact with TheraCal and ProRoot MTA for 7 days in DPBS or (b) 14 days in HBSS.

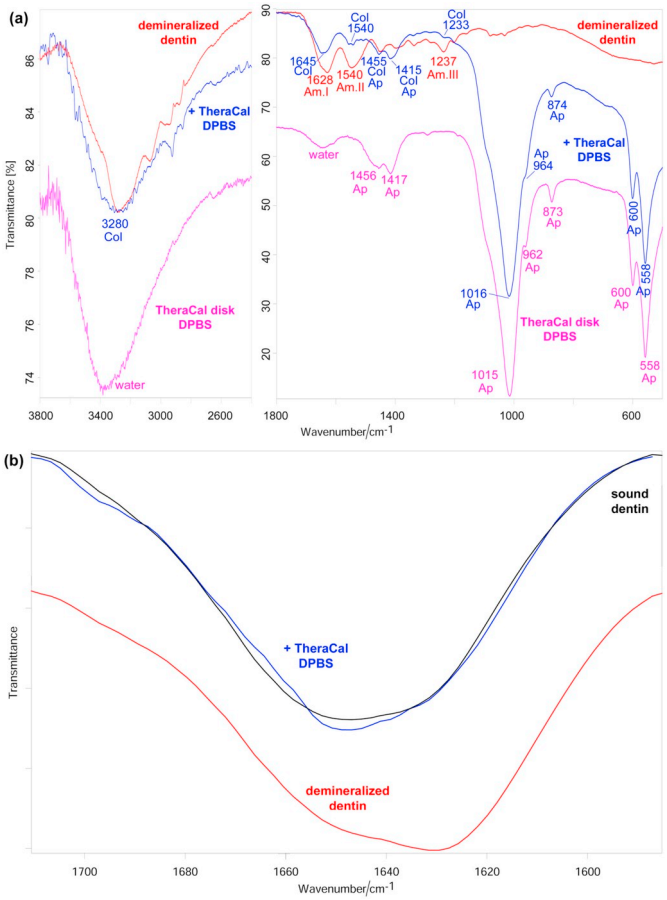

Fig. 4. (a) Average IR spectra recorded on the demineralized dentin slices before and after ageing in contact with TheraCal for 7 days in DPBS. The spectra were normalized to the intensity of the Amide A band at about 3280 cm^{-1}. The spectrum recorded on the aged TheraCal disk is reported for comparison. The bands prevalently due to collagen (Col) and B-type carbonated apatite (Ap) are indicated. (b) Average IR spectra in the Amide I range recorded on the demineralized dentin slices before and after ageing in contact with TheraCal for 7 days in DPBS. The spectrum of sound dentin is reported for comparison.

the deposit formed on the corresponding cement disk (Fig. 7(c)).

Also upon remineralization in HBSS, the collagen Amide I, II and III bands underwent shifts in their wavenumber positions (Figs. 8, 9 and 10) and changes in relative intensities analogous to those observed in DPBS, although less significant; upon remineralization, the Amide I profile remained more similar to demineralized dentin than sound dentin (Figs. 8(b) and 9(b)). The band fitting procedure (see Fig. S3, Supplementary Information, for the fitted spectra) showed that upon remineralization in HBSS, the collagen triple-helix content of sound dentin was recovered (Fig. 3(b)), while the amounts of the other conformations (in particular, β-sheet and α-helix) were significantly different.

Figs. S4 and S5, Supplementary Information, show the average IR spectra of demineralized dentin slices before and after ageing for 14 days in HBSS and in the calcifying solution according to Chirila et al. [34], respectively. No significant remineralization was observed under these conditions.

4. Discussion

4.1. Dentin demineralization

Vibrational spectroscopy proved suitable to characterize the collagen demineralization and remineralization processes as well as the phases formed on the cement disks upon soaking in SBFs. EDTA has been chosen as demineralizing agent since it is usually used in endodontic therapy to remove smear layer and dentin debris and to demineralize the dentine surface and remove bacteria from the root canal space [25,26]. EDTA irrigation is usually used for 20–60 min and may be repeated for 2–3 clinical appointments. After irrigation, root canal must be filled with MTA or other similar materials (such as Dycal or TheraCal) to prevent any further root fracture and cracks caused by changes in dentin architecture and composition induced by EDTA. In the present study, the EDTA treatment has been chosen as a simple experimental model to create the typical conditions obtained during the endodontic therapy. On the other hand, EDTA creates a simple and well reproducible substrate to observe the chemical modifications induced by the following treatment with different cement materials.

ATR-IR spectroscopy showed that the EDTA treatment used in the present study was able to demineralize dentin down to its first 2 μm of thickness, at least. Actually, as observable in Fig. 1, the bands assignable to B-type carbonated apatite completely disappeared and the $I_{apatite}/I_{collagen}$ ratio (Fig. 7(b)) significantly decreased. These measurements were in agreement with the previously reported ESEM-EDX analyses that did not show any trace of Ca and P peaks on demineralized dentin slices obtained under the same conditions [40]. Moreover, EDX depth profile on fractured demineralized dentin sections proved that the treatment used completely removed the mineral phase of dentin to approx. 50 μm depth [40]. On the other hand, FT-Raman spectroscopy, which is more sensitive to the sample bulk, showed that under the utilized conditions, dentin demineralized only partially. In fact, as observable from the average FT-Raman spectrum of the demineralized dentin slices (Fig. 2), the B-type carbonated apatite bands were still detected, suggesting that this phase was still present in the sample bulk. Therefore, the demineralizing treatment interested only the surface of the specimens.

The changes observed in the relative intensity of the IR Amide bands (Fig. 1) may be related to the loss of interactions between collagen (in particular through its C═O groups) and Ca^{2+} ions upon

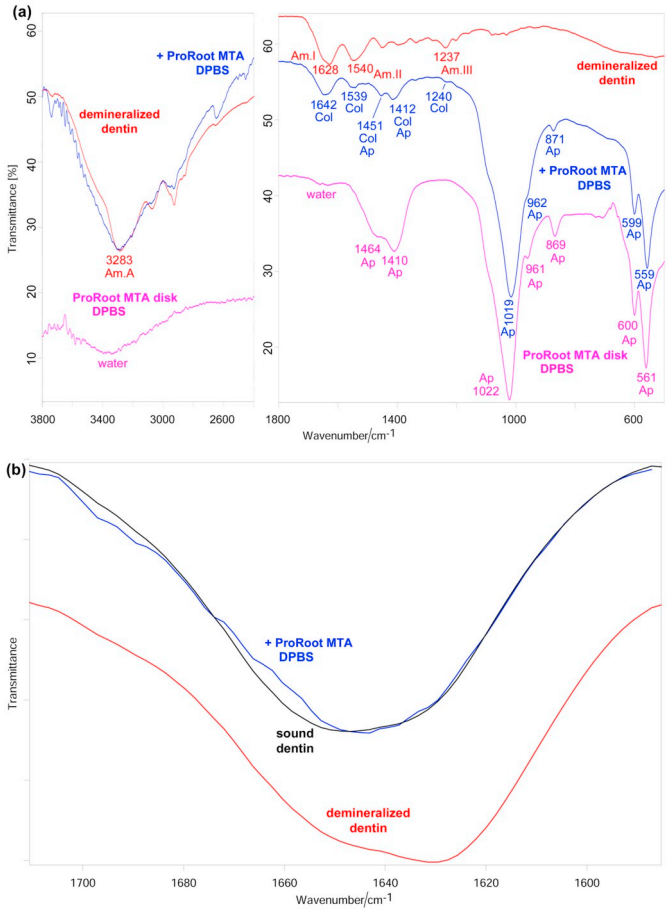

Fig. 5. (a) Average IR spectra recorded on the demineralized dentin slices before and after ageing in contact with ProRoot MTA for 7 days in DPBS. The spectra were normalized to the intensity of the Amide A band at about 3280 cm^{-1}. The spectrum recorded on the aged ProRoot MTA disk is reported for comparison. The bands prevalently due to collagen (Col) and B-type carbonated apatite (Ap) are indicated. (b) Average IR spectra in the Amide I range recorded on the demineralized dentin slices before and after ageing in contact with ProRoot MTA for 7 days in DPBS. The spectrum of sound dentin is reported for comparison.

demineralization, according to previous studies [41,42]. These interactions appeared of key importance in order that collagen assumes its triple-helix structure as well as its characteristic hydrogen bonding pattern. Actually, the increase of the $I_{Amide\ II}/I_{Amide\ I}$ ratio upon treatment with EDTA (Fig. 7(a)) may be interpreted as a sign of a changed hydrogen bonding arrangement after demineralization. On the other hand, the value of the $I_{Amide\ III}/I_{1450}$ ratio in demineralized dentin (lower than 1) suggests that the integrity of the triple-helix is affected to a certain extent. These findings were confirmed by the Amide I fitting data. As observable from Fig. 3, in sound dentin the main collagen conformation was triple-helix, as expected. Demineralization significantly altered the secondary structure distribution: after treatment with EDTA, the prevailing secondary structure became β-sheet and the content of unordered conformation increased as well at the expenses of triple-helix, α-helix and β-turns.

4.2. Remineralization tests

In spite of the above reported structural rearrangements, collagen did not lose its ability to chelate calcium ions under remineralizing conditions (i.e. upon treatment with the cements in SBF solutions). In this context, it may be observed that the β-sheet conformation (i.e. the prevailing one in demineralized dentin, Fig. 2(b)) has been identified as a particularly advantageous structured surface for mineral induction [3,43,44]. It is interesting to note that, under remineralizing conditions, the $I_{Amide\ II}/I_{Amide\ I}$ ratio decreased again towards the values observed in sound dentin (Fig. 7(a)). The Amide I fitting data showed that, upon remineralization in both DPBS and HBSS, the triple-helix content of sound dentin was nearly recovered (Fig. 3(a) and (b)), whilst the α-helix content was lower than in sound dentin. Moreover, it must be stressed that upon treatment in DPBS, the β-sheet conformation attained the amount present in sound dentin (Fig. 3(a)), whilst did not in HBSS (Fig. 3(b)). These trends would suggest that the interactions with calcium ions under remineralizing conditions allowed collagen to rearrange into a conformation similar to that of native dentin and this process appeared more delayed in HBSS than DPBS. This result does not appear unexpected and reflects the different degrees of maturation of the inorganic phase deposited onto dentin in the two soaking media. In fact, demineralized dentin enucleated a B-type carbonated apatite upon treatment with all the cements in DPBS (Figs. 4–6); on the contrary, upon soaking in HBSS, this phase formed only in presence of TheraCal (Fig. 8), but was less crystalline (i.e. less mature) than in DPBS, since it

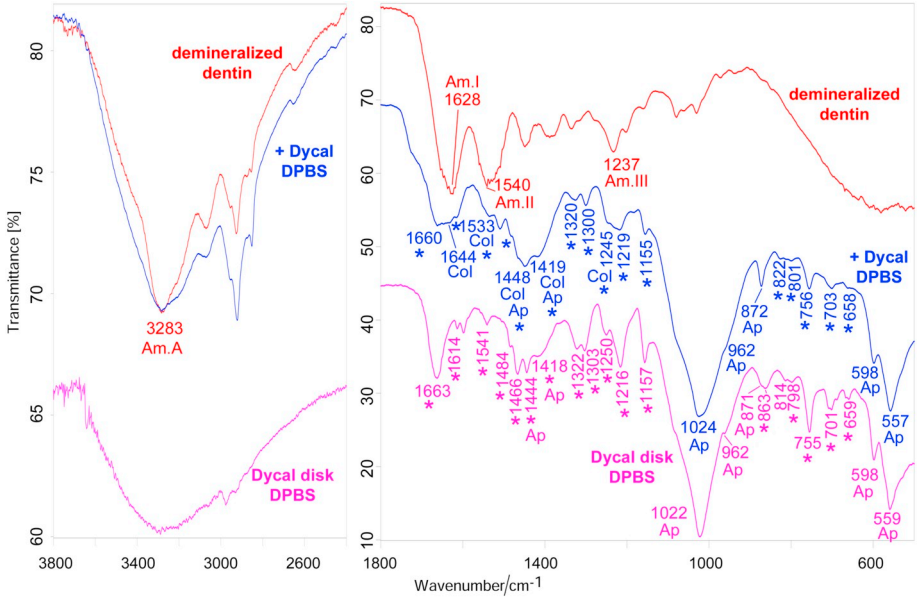

Fig. 6. Average IR spectra recorded on the demineralized dentin slices before and after ageing in contact with Dycal for 7 days in DPBS. The spectra were normalized to the intensity of the Amide A band at about 3280 cm^{-1}. The spectrum recorded on the aged Dycal disk is reported for comparison. The bands prevalently due to collagen (Col) and B-type carbonated apatite (Ap) are indicated as well as those assignable to the salicylate component belonging to the cement (*).

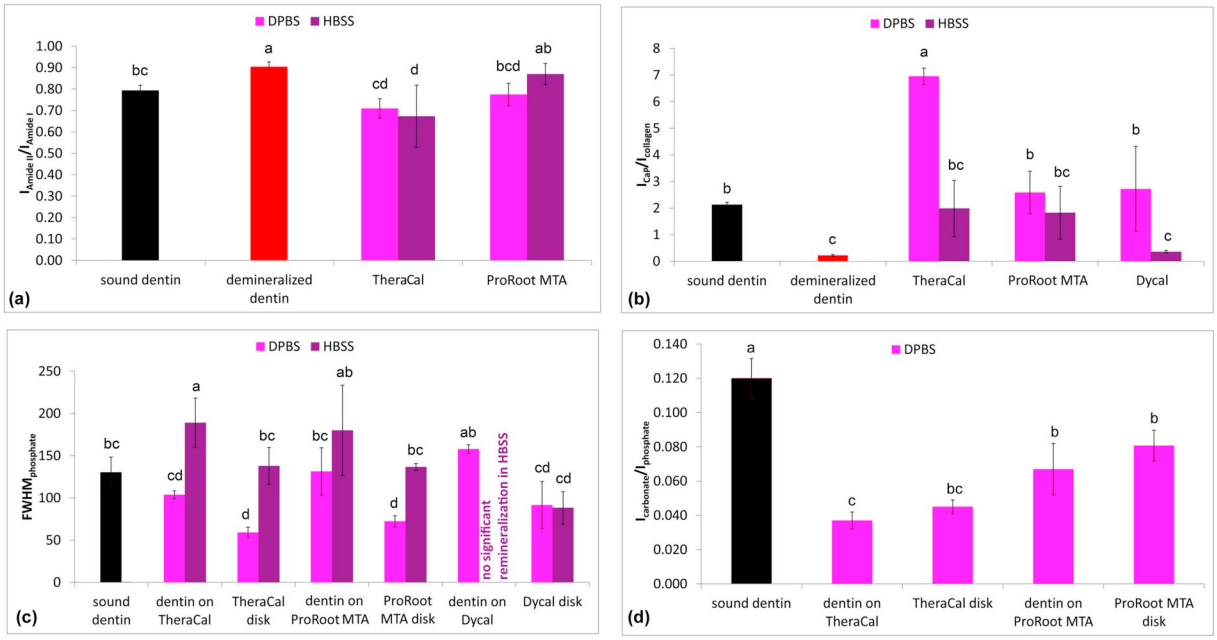

Fig. 7. (a) Values of the $I_{Amide\ II}/I_{Amide\ I}$ ratio (average ± standard deviation) as calculated from the IR spectra of sound dentin, demineralized dentin slices before and after ageing in contact with TheraCal and ProRoot MTA in DPBS and HBSS. Values (average ± standard deviation) of (b) the $I_{CaP}/I_{collagen}$ intensity ratio, (c) full-width at half maximum of the ν_3 PO_4^{3-} band ($FWHM_{phosphate}$), (d) $I_{carbonate}/I_{phosphate}$ ratio calculated from the IR spectra recorded on sound and demineralized dentin as well as on the demineralized dentin slices that stayed in contact with TheraCal, ProRoot MTA and Dycal for 7 days in DPBS and 14 days in HBSS. In the histogram (d), the data corresponding to Dycal as well as to the HBSS medium were not reported due to the significant contribution of the salicylate component and calcite, respectively, to the 870 cm^{-1} band. Different letters on the histogram bars represent statistically significant differences ($p < 0.05$).

was characterized by a significantly higher $FWHM_{phosphate}$ (Fig. 7(c)). In presence of ProRoot MTA (Fig. 9), a still less mature ACP phase was enucleated. With Dycal no significant remineralization was detected (Fig. 10). These trends suggest that TheraCal and Dycal were the most and least active remineralizing agents, respectively; this result is not surprising since data previously reported [28] showed that TheraCal released statistically more calcium ions than both ProRoot MTA and Dycal throughout the whole tested period (3 h–28 d).

The $I_{CaP}/I_{collagen}$ ratio, identified as a marker of the CaP thickness, confirmed these trends: for the highest and lowest remineralizing agents (i.e. TheraCal and Dycal, respectively) significant differences were found between the $I_{CaP}/I_{collagen}$ ratios measured in DPBS and HBSS (Fig. 7(b)), with values higher in the former than in the latter. These results demonstrated that, in HBSS, as stressed above, the mineralization process is delayed, since the deposit formed was less mature and thinner, in agreement with previous studies [16]. This behavior may be explained in relation to the different composition of the two SBF media. DPBS is a physiological-like buffered (pH 7.4) Ca^{2+}-, Mg^{2+}- and HCO_3^--free solution with 9.56 mM PO_4^{3-} concentration, whilst HBSS is a Ca^{2+}-, Mg^{2+}- and HCO_3^--containing simulated body fluid with 0.776 mM PO_4^{3-} concentration. The lower degree of maturation of the inorganic phase enucleated in the HBSS medium may be explained in relation to the significantly lower PO_4^{3-} content of this medium, as well as to the influence of Mg^{2+} ions, which have been reported to kinetically stabilize the ACP phase [45] and to inhibit apatite crystallization [46]. At the same time, upon soaking in HBSS, high amounts of calcium carbonate (as calcite and aragonite) were found to form on the cements surface (Figs. 8, 9 and 10). This behavior, not observed upon ageing in DPBS (Figs. 4, 5 and 6), may be related to the presence of bicarbonate ions in the former medium. Actually, under these conditions, the apatite crystallization has been reported to be affected [45].

It is well known that type I collagen, the main matrix protein in dentin, forms enclosed spaces where the mineral phase grows. When the degree of supersaturation of calcium and phosphate ions is high, apatite, i.e. the phase thermodynamically more stable, is formed via intermediate amorphous precursors (ACP). They infiltrate into the nanoscopic gaps of collagen fibrils through electrostatic attraction, capillary action and size exclusion [47] and further transform into platy nanocrystalline apatite [9,48]. It is interesting to note that the dentin slices demineralized under the experimental conditions here reported were not able to remineralize upon soaking for 14 days either in HBSS (Fig. S4, Supplementary Information) or in the calcifying solution according to Chirila et al. [34] (Fig. S5, Supplementary Information), i.e. without any cement. This subject is under debate, as well as the role of collagen in biomineralization. Some authors have reported that demineralized dentin remineralizes when placed in solutions that are metastable with respect to hydroxyapatite and have related this ability to the phosphate ester bound to collagen [49]. Other studies have described a negligible dentin remineralization in SBF solutions [7,50]. It has been reported that type I collagen matrix is not able to initiate apatite nucleation from metastable calcium phosphate solutions that do not spontaneously precipitate [1]. Type I collagen defines the space for crystal deposition, its size and morphology, while non-collagenous matrix macromolecules (such as DMP1) are involved in the nucleation, transformation and growth of the mineral phase. On the contrary, more recent studies have reported that type I collagen in vitro can initiate and orientate the growth of carbonated apatite in the absence of any other vertebrate extracellular matrix molecules of calcifying tissues, questioning the need of mediation by NCP for collagen mineralization to occur in vivo [51–53].

From the results of our study, it is evident that the adopted demineralization conditions did not alter collagen structure to such an extent to prevent remineralization. On the other hand, it must be stressed that the demineralized dentin samples used in the present study were only partially demineralized (Fig. 2). Therefore, a possible role played by the residual crystals present after demineralization cannot be excluded since the elution of substances from the underlying mineralized dentin may trigger the remineralization process [10,54]. In other words, besides calcium chelation by collagen revealed by IR spectroscopy, growth of residual crystals may occur [55]. Wang et al. [56] have

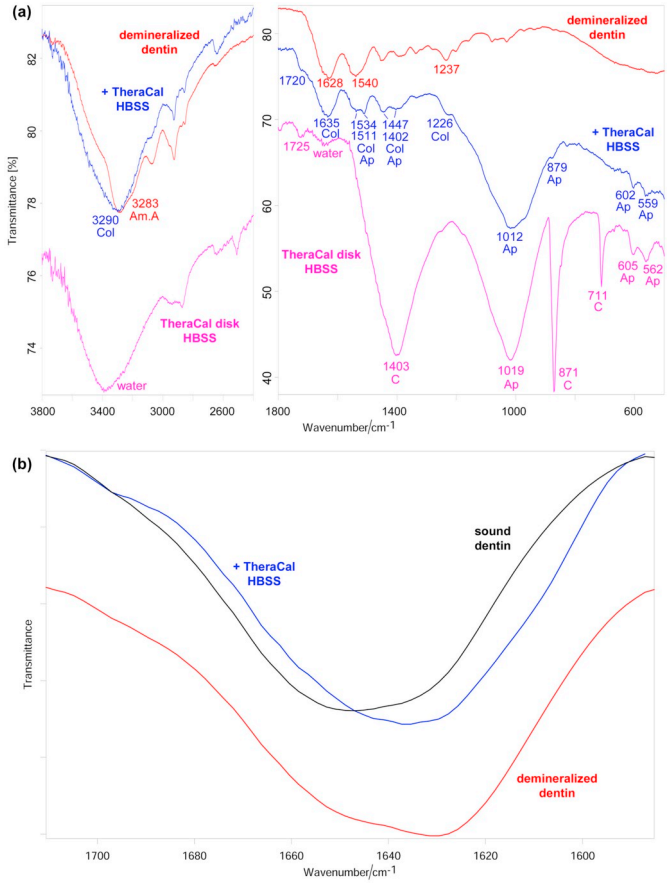

Fig. 8. (a) Average IR spectra recorded on the demineralized dentin slices before and after ageing in contact with TheraCal for 14 days in HBSS. The spectra were normalized to the intensity of the Amide A band at about 3280 cm^{-1}. The spectrum recorded on the aged TheraCal disk is reported for comparison. The bands prevalently due to collagen (Col), B-type carbonated apatite (Ap) and calcite (C) are indicated. (b) Average IR spectra in the Amide I range recorded on the demineralized dentin slices before and after ageing in contact with TheraCal for 14 days in HBSS. The spectrum of sound dentin is reported for comparison.

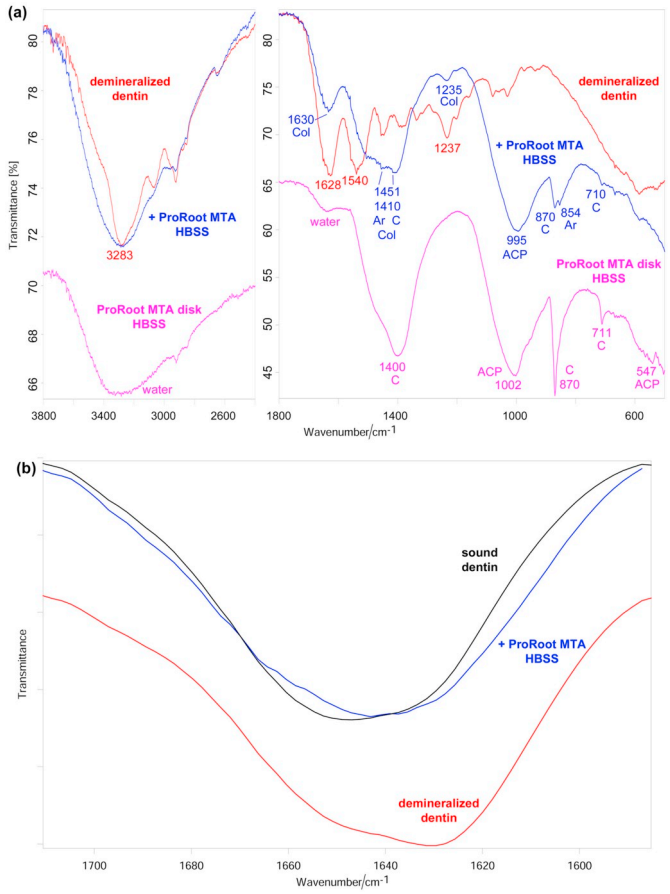

Fig. 9. (a) Average IR spectra recorded on the demineralized dentin slices before and after ageing in contact with ProRoot MTA for 14 days in HBSS. The spectra were normalized to the intensity of the Amide A band at about 3280 cm^{-1}. The spectrum recorded on the aged ProRoot MTA disk is reported for comparison. The bands prevalently due to collagen (Col), amorphous calcium phosphate (ACP), calcite (C) and aragonite (Ar) are indicated. (b) Average IR spectra in the Amide I range recorded on the demineralized dentin slices before and after ageing in contact with ProRoot MTA for 14 days in HBSS. The spectrum of sound dentin is reported for comparison.

observed that the remineralization effect on completely demineralized dentin was weaker than on partially demineralized dentin. They have ascribed this behaviour to the absence of dentin mineral contribution and difficulty in crystal nucleation. The rationale behind using partially and completely demineralized models in that study was based on the elimination of the ambiguity in differentiating the remineralized apatite crystallites from remnant apatite seed crystallites existing in partially demineralized dentine [53]. The completely demineralized dentine may ascertain that remineralization was able to occur without a contribution from NCP and proteoglycans released from mineralized dentine [53]. In our study, we have preferred to use partially demineralized dentin, which is the clinical situation usually obtained after the use of EDTA solutions in endodontic therapy.

In any case, remineralization was found to be strongly dependent on the presence of the cements and their calcium releasing ability, since in their absence no remineralization was observed (Fig. S4, Supplementary Information); evidently, with decreasing medium saturation, the time required for mineral induction increases and no deposit was detected. Increasing the concentration of the main inorganic ions of the apatite phase (Ca^{2+} in particular, due to their release from the cements) has an impact on the resulting mineralization [51]. Actually, it is well known that changes in extracellular calcium ion concentrations affect bone formation and remodeling, and more in general the biomineralization processes [57,58]. Recent in vitro studies have shown that calcium concentration affects the degree of collagen self-assembly as well as the extent of mineralization, being the latter phenomenon improved at high calcium concentrations [59].

It is interesting to note that also the organic components of the TheraCal and Dycal cements appeared to play a role in dentin remineralization. The average IR spectrum recorded on the demineralized dentin slices that stayed in contact with TheraCal in HBSS (Fig. 8) showed a broad band at about 1720 cm^{-1}, ascribable to the C=O stretching mode of the polymeric phase. This result shows that in the earlier phases of remineralization (in HBSS this process is delayed), also the C=O groups of the resin may participate in calcium chelation, according to previous studies [32]. The salicylate component was detected on the dentin slices that stayed in contact with Dycal in DPBS, i.e. under conditions that induced apatite deposition (Fig. 6). This result is not unexpected, since the calcium chelating ability of salicylate has been described [44].

As previously reported [32], the above discussed IR findings showed that collagen network underwent conformational rearrangements upon remineralization. The calcium phosphate phases rather than simple deposits, appeared intimately bound to the collagen matrix, a situation which has been reported to facilitate the recovery of the mechanical properties of the tissue [60]. In fact, the spectra of the newly formed inorganic phases were different from those recorded on the corresponding aged cement disks (which were analogous to those of the

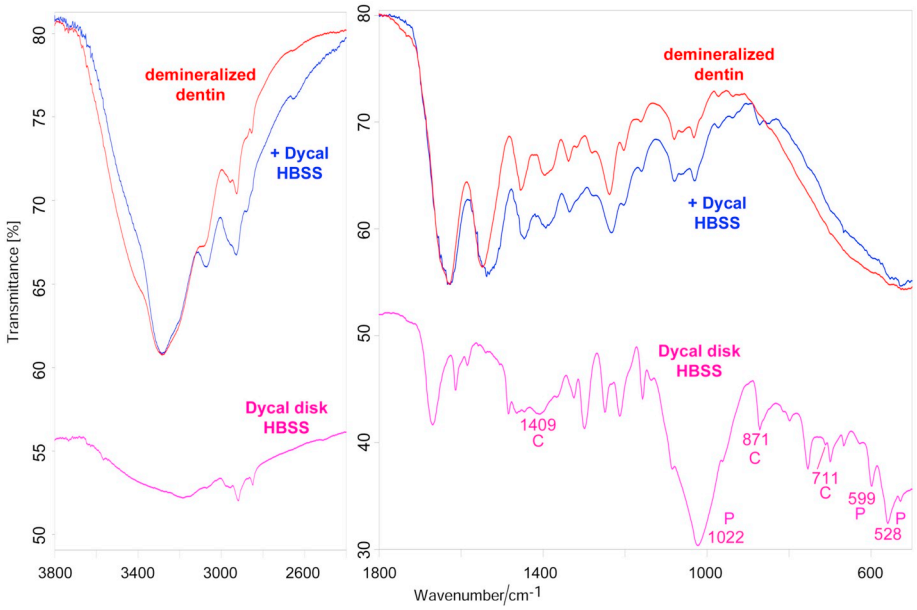

Fig. 10. Average IR spectra recorded on the demineralized dentin slices before and after ageing in contact with Dycal for 14 days in HBSS. The spectra were normalized to the intensity of the Amide A band at about 3280 cm^{-1}. The spectrum recorded on the aged Dycal disk is reported for comparison. The bands prevalently due to calcite (C) and calcium phosphate belonging to the cement (P) are indicated.

powders obtained from the soaking media, not shown). In this regard, it must be observed that the IR spectra of all the remineralized dentin slices still showed the bands of collagen, suggesting that in the surface skin of the samples (i.e. in the first 2 μm), collagen and CaP coexisted.

The phase enucleated by demineralized dentin upon soaking in the presence of the cements in DPBS or HBSS had a meanly lower crystallinity (i.e. a meanly higher $FWHM_{phosphate}$, Fig. 7(c)) than the phase formed on the corresponding material disk (Figs. 4–6 and 8, 9). Moreover, the carbonate content of the B-type carbonated apatite phase enucleated by demineralized dentin in DPBS was meanly lower than in the deposit formed on the corresponding TheraCal and ProRoot MTA disks (Figs. 4, 5, 7(d)). However, the high standard deviation associated to the $I_{carbonate}/I_{phosphate}$ values made the differences not statistically significant. In this context, it must be recalled that carbonate naturally substitutes into the apatite lattice over time, and the total carbonate content and crystallinity of the mineralized tissues increases with age/maturation [61]. The results of our study suggest that collagen should act as a spatial constraint to crystal deposition, affecting the morphology (i.e. crystallinity) of the enucleated phase as well as its carbonate content. Actually, it has been reported that, the amorphous-crystalline transformation is retarded in the presence of collagen in comparison to the calcium phosphate formation without collagen [62], suggesting a mineralization inhibitor role for collagen, a highly debated subject for decades [63]. Moreover, the synergistic role of recombinant collagen and Mg^{2+} ions in stabilizing the ACP phase and inhibiting apatite crystal growth has been recently reported [45].

Considering that ProRoot MTA, Dycal and TheraCal showed a prolonged calcium release [28] and promote the formation of an apatite biocoating, both these conditions may play active roles in vivo in up-regulating pulp cell gene expression to induce mineralized tissue formation. Moreover, the nucleation of apatite spherulites at the interface may enhance the sealing of the dentin/material interspace, thereby representing a critical factor to ensure the seal of the dental pulp complex and prevent any further leakage.

5. Conclusions

Vibrational spectroscopy proved suitable to investigate at a molecular level the dentin demineralization and remineralization processes. The EDTA treatment used in this study to demineralize dentin significantly altered the secondary structure distribution of collagen: the prevailing secondary structure became β-sheet, instead of triple-helix. However, collagen did not lose its ability to chelate calcium ions under remineralizing conditions (i.e. upon treatment with the cements in DPBS or HBSS). The interactions with calcium ions under remineralizing conditions allowed collagen to rearrange into a conformation similar to that of sound dentin and this process appeared slower in HBSS than DPBS, as also shown by the lower degree of maturation of the inorganic phase enucleated in the former medium (amorphous calcium phosphate in HBSS versus B-type carbonated apatite in DPBS). Collagen appeared to act as a spatial constraint to crystal deposition, affecting crystallinity and carbonate content of the enucleated phase. Remineralization was found to strongly depend on the calcium releasing ability of the cements; actually, this phenomenon was not observed upon soaking in HBSS. The organic phases of TheraCal and Dycal (through C═O and COO^- groups) seemed to play a role in dentin remineralization. The fast formation of a rough apatite biocoating may represent a favorable clinical condition in the context of mineralized tissue regeneration.

Abbreviations

EDTA	ethylenediaminetetraacetic acid
DPBS	Dulbecco's Phosphate Buffered Saline
HBSS	Hank's Balanced Salt Solution
NCP	non-collagenous proteins
DMP1	dentin matrix protein 1
DPP	dentin phosphoprotein
MTA	mineral trioxide aggregate
SBF	simulated body fluid
PVC	polyvinyl chloride
ATR	attenuated total reflectance
FT	Fourier Transform
UDMA	urethane dimethacrylate
BisGMA	bisphenol A-glycidyl methacrylate
TEGDMA	triethylene glycol dimethacrylate
HEMA	hydroxyethyl methacrylate
PEGDMA	polyethylene glycol dimethacrylate
DTGS	deuterated triglycine sulphate
Nd^{3+}-YAG	neodymium-doped yttrium aluminum garnet
ACP	amorphous calcium phosphate
FWHM	full-width at half maximum

Declarations of interest

None.

Acknowledgements

This work was supported by RFO funds from University of Bologna. The founding sponsor had no role in the design of the study; in the collection, analyses, or interpretation of data; in the writing of the manuscript, and in the decision to submit the article for publication.

Conflicts of interest

None.

Appendix A. Supplementary data

Supplementary data to this article can be found online at https://doi.org/10.1016/j.jinorgbio.2019.01.004.

References

[1] S. Gajjeraman, K. Narayanan, J. Hao, C. Qin, A. George, J. Biol. Chem. 282 (2007) 1193–1204.
[2] E. Beniash, Wiley Interdiscip. Rev. Nanomed. Nanobiotechnol. 3 (2011) 47–69.
[3] G. He, T. Dahl, A. Veis, A. George, Nat. Mater. 2 (2003) 552–558.
[4] A. George, A. Veis, Chem. Rev. 108 (2008) 4670–4693.
[5] M. Nakajima, S. Kunawarote, T. Prasansuttiporn, J. Tagami, Japan. Dent. Sci. Rev. 47 (2011) 102–114.
[6] Z. Xu, K.G. Neoh, C.C. Lin, A. Kishen, J. Biomed. Mater. Res. B 98B (2011) 150–159.
[7] T.Y. Ning, X.H. Xu, L.F. Zhu, X.P. Zhu, C.H. Chu, L.K. Liu, Q.L. Li, J. Biomed. Mater. Res., Part B 100B (2012) 138–144.
[8] Y.K. Kim, L. Gu, T.E. Bryan, J.R. Kim, L. Chen, Y. Liu, J.C. Yoon, L. Breschi, D.H. Pashley, F.R. Tay, Biomaterials 31 (2010) 6618–6627.
[9] L.B. Gower, Chem. Rev. 108 (2008) 4551–4627.
[10] F.R. Tay, D.H. Pashley, Biomaterials 29 (2008) 1127–1137.
[11] L. Niu, S.E. Jee, K. Jiao, L. Tonggu, M. Li, L. Wang, Y. Yang, J. Bian, L. Breschi, S. Soon, J.J. Chen, D.H. Pashley, F.R. Tay, Nat. Mater. 16 (2017) 370–378.
[12] F.R. Tay, D.H. Pashley, F.A. Rueggeberg, R.J. Loushine, R.N. Weller, J. Endod. 33 (2007) 1347–1351.
[13] M.G. Gandolfi, P. Taddei, A. Tinti, E. Dorigo De Stefano, C. Prati, Mater. Sci. Eng. C 31 (2011) 1412–1422.
[14] M.G. Gandolfi, P. Taddei, A. Tinti, C. Prati, Int. Endod. J. 43 (2010) 917–929.
[15] N.J. Coleman, J.W. Nicholson, K. Awosanya, Cem. Concr. Res. 37 (2007) 1518–1523.
[16] P. Taddei, A. Tinti, M.G. Gandolfi, P.L. Rossi, C. Prati, J. Raman Spectrosc. 40 (2009) 1858–1866.
[17] J.F. Reyes-Carmona, A.R.S. Santos, C.P. Figueiredo, M.S. Felippe, W.T. Felippe, M.M. Cordeiro, J. Endod. 37 (2011) 731–736.
[18] M.G. Gandolfi, F. Perut, G. Ciapetti, P. Taddei, E. Modena, P.L. Rossi, C. Prati, J. Appl. Biomater. Biomech. 7 (2009) 160–170.
[19] T. Takita, M. Hayashi, O. Takeichi, B. Ogiso, N. Suzuki, K. Otsuka, K. Ito, Int. Endod. J. 39 (2006) 415–422.
[20] S. Maeno, Y. Niki, H. Matsumoto, H. Morioka, T. Yatabe, A. Funayama, Y. Toyama, T. Taguchi, J. Tanaka, Biomaterials 26 (2005) 4847–4855.
[21] O. Tecles, P. Laurent, V. Aubut, I. About, J. Biomed. Mater. Res., Part B 85B (2008) 180–187.
[22] T.E. Bryan, K. Khechen, M.G. Brackett, R.L.W. Messer, A. El-Awady, C.M. Primus, J.L. Gutmann, F.R. Tay, J. Endod. 36 (2010) 1163–1169.
[23] M.D. Accorinte, R. Holland, A. Reis, M.C. Bortoluzzi, S.S. Murata, E. Dezan Jr., V. Souza, L.D. Alessandro, J. Endod. 34 (2008) 1–6.
[24] P.N. Nair, H.F. Duncan, T.R. Pitt Ford, H.U. Luder, Int. Endod. J. 41 (2008) 128–150.
[25] A. Serper, S. Calt, J. Endod. 28 (2002) 501–502.
[26] F.R. Tay, J.L. Gutmann, D.H. Pashley, J. Endod 33 (2007) 1086–1090.
[27] C. de Carvalho Almança Lopes, P.H.J. Oliveira Limirio, V. Resende Novais, P. Dechichi, Appl. Spectrosc. Rev. 53 (2018) 747–769.
[28] M.G. Gandolfi, F. Siboni, C. Prati, Int. Endod. J. 45 (2012) 571–579.
[29] E. Goormaghtigh, J.-M. Ruysschaert, V. Raussens, Biophys. J. 90 (2006) 2946–2957.
[30] D.M. Byler, H. Susi, Biopolymers 25 (1986) 469–487.
[31] B. Ram Singh, Chapter 1 basic aspects of the technique and applications of infrared spectroscopy of peptides and proteins, Analysis of Peptides and Proteins ACS Symposium Series, American Chemical Society, Washington, DC, 1999.
[32] P. Taddei, C. Prati, M.G. Gandolfi, Mater. Sci. Eng. C 77 (2017) 755–764.
[33] J.M. Very, R. Gibert, B. Guilhot, M. Debout, C. Alexandre, Calcif. Tissue Int. 60 (1997) 271–275.
[34] T.V. Chirila, D.A. Morrison, Z. Gridneva, A.J. Garcia, S.T. Platten, B.J. Griffin, A.K. Zainuddin, D.J.T. Whittaker, J. Hill, Mater. Sci. Lett. 24 (2005) 4987–4990.
[35] T. Du, X. Niu, Z. Li, P. Li, Q. Feng, Y. Fan, Int. J. Biol. Macromol. 113 (2018) (450–45).
[36] L. Shen, H. Bu, H. Yang, W. Liu, G. Li, Int. J. Biol. Macromol. 115 (2018) 635–642.
[37] X. Liu, N. Dan, W. Dan, Int. J. Biol. Macromol. 88 (2016) 179–188.
[38] N.P. Camacho, C.M. Rimnac, R.A. Meyer Jr., S. Doty, A.L. Boskey, Bone 17 (1995) 271–278.
[39] D.G.A. Nelson, J.D.B. Featherstone, Calcif. Tissue Int. 34 (1982) S69–S81.
[40] M.G. Gandolfi, P. Taddei, F. Siboni, E. Modena, E. Dorigo De Stefano, C. Prati, Dent. Mater. 27 (2011) 1055–1069.
[41] W. Zhang, Z.L. Huang, S.S. Liao, F.Z. Cui, J. Am. Ceram. Soc. 86 (2003) 1052–1054.
[42] B. Ye, X. Luo, Z. Li, C. Zhuang, L. Li, L. Lu, S. Ding, J. Tian, C. Zhou, Mater. Sci. Eng. C 68 (2016) 43–51.
[43] A. Takeuchi, C. Ohtsuki, M. Kamitakahara, S. Ogata, M. Tanihara, T. Miyazaki, Key Eng. Mater. 309-311 (2006) 489–492.
[44] S. Dahlin, J. Angstrom, A. Linde, Eur. J. Oral Sci. 106 (1998) 239–248.
[45] G.B. Ramírez-Rodríguez, J.M. Delgado-López, M. Iafisco, M. Montesi, M. Sandri, S. Sprio, A. Tampieri, J. Struct. Biol. 196 (2016) 138–146.
[46] B. Bracci, P. Torricelli, S. Panzavolta, E. Boanini, R. Giardino, A. Bigi, J. Inorg. Biochem. 103 (2009) 1666–1674.
[47] K. Jiao, L. Niu, C.F. Ma, X.Q. Huang, D.D. Pei, T. Luo, Q. Huang, J.H. Chen, F.R. Tay, Adv. Funct. Mater. 26 (2016) 6858–6875.
[48] F. Nudelman, A.J. Lausch, N.A.J.M. Sommerdijk, E.D. Sone, J. Struct. Biol. 183 (2013) 258–269.
[49] T. Saito, M. Yamauchi, M.A. Crenshaw, J. Bone Miner. Res. 13 (1998) 265–270.
[50] K. Kawasaki, J. Ruben, I. Stokroos, O. Takagi, J. Arends, Caries Res. 33 (1999) 275–280.
[51] Y. Wang, T. Azaïs, M. Robin, A. Vallée, C. Catania, P. Legriel, G. Pehau-Arnaudet, F. Babonneau, M.M. Giraud-Guille, N. Nassif, Nat. Mater. 11 (2012) 724–733.
[52] F.H. Silver, W.J. Landis, Connect. Tissue Res. 52 (2011) 242–254.
[53] L.S. Gu, B.P. Huffman, D.D. Arola, Y.K. Kim, S. Mai, M.E. Elsalanty, J. Ling, D.H. Pashley, F.R. Tay, Acta Biomater. 6 (2009) 1453–1461.
[54] M. Balooch, S. Habelitz, J.H. Kinney, S.J. Marshall, G.W. Marshall, J. Struct. Biol. 162 (2008) 404–410.
[55] P.G. Koutsoukos, G.H. Nancollas, J. Cryst. Growth 53 (1981) 10–19.
[56] Z. Wang, T. Jiang, S. Sauro, Y. Wang, I. Thompson, T.F. Watson, Y. Sa, W. Xing, Y. Shen, M. Haapasalo, J. Dent. 39 (2011) 746–756.
[57] M.M. Dvorak, A. Siddiqua, D.T. Ward, D.H. Carter, S.L. Dallas, E.F. Nemeth, D. Riccardi, Proc. Natl. Acad. Sci. U. S. A. 101 (2004) 5140–5145.
[58] R. Sunarso, K. Toita, K. Ishikawa Tsuru, Mater. Sci. Eng. C 68 (2016) 291–298.
[59] X. Niu, R. Fan, F. Tian, X. Guo, P. Li, Q. Feng, Y. Fan, Mater. Sci. Eng. C 73 (2017) 137–143.
[60] L.E. Bertassoni, S. Habelitz, J.H. Kinney, S.J. Marshall, G.W. Marshall Jr, Caries Res. 43 (2009) 70–77.
[61] R. Legros, N. Balmain, G. Bonel, Calcif. Tissue Int. 41 (1987) 137–144.
[62] J.H. Bradt, M. Mertig, A. Teresiak, W, Chem. Mater. 11 (1999) 2694–2701.
[63] A.L. Boskey, Connect. Tissue Res. 35 (1996) 357–363.